European Journal of Pharmaceutics and Biopharmaceutics 73 (2009) 292–301

Contents lists available at ScienceDirect

European Journal of Pharmaceutics and Biopharmaceutics

journal homepage: www.elsevier.com/locate/ejpb

Research paper

Modeling drug release from hot-melt extruded mini-matrices with constant and non-constant diffusivities

E. Verhoeven [a], F. Siepmann [b], T.R.M. De Beer [c], D. Van Loo [d], G. Van den Mooter [e], J.P. Remon [a], J. Siepmann [b], C. Vervaet [a,*]

[a] Laboratory of Pharmaceutical Technology, Ghent University, Gent, Belgium
[b] College of Pharmacy, University of Lille, Lille, France
[c] Department of Pharmaceutical Analysis, Ghent University, Gent, Belgium
[d] Ghent University Centre for X-ray Tomography (UGCT), Ghent University, Gent, Belgium
[e] Laboratory of Pharmacotechnology and Biopharmacy, University of Leuven, Leuven, Belgium

ARTICLE INFO

Article history:
Received 12 January 2009
Accepted in revised form 16 June 2009
Available online 21 June 2009

Keywords:
Mathematical modeling
Hot-melt extrusion
Controlled release
Diffusion
Ethylcellulose

ABSTRACT

Different types of ethylcellulose-based mini-matrices were prepared by hot-melt extrusion and thoroughly characterized in vitro. Metoprolol tartrate was used as model drug, and various amounts and types of polyethylene glycol (PEG)/polyethylene oxide (PEO) were added as release rate modifiers. Based on the experimental results, appropriate mathematical theories were identified/developed, allowing for a better understanding of the underlying drug release mechanisms. For instance, it could be shown that at high initial PEG/PEO contents and/or intermediate initial PEG/PEO contents of low molecular weight, drug diffusion with time- and position-independent diffusivities is predominant. In contrast, at low initial PEG/PEO contents and intermediate initial PEG/PEO contents of high molecular weight, the time- and position-dependent dynamic changes in the matrix porosities significantly affect the conditions for drug and PEG/PEO diffusion. These dynamic changes must be taken into account in the mathematical model. Importantly, the proposed theories are mechanistic realistic and also allow for the quantitative prediction of the effects of the device design on the resulting drug release patterns. Interestingly, these quantitative predictions could be confirmed by independent experiments. Furthermore, Raman spectroscopy allowed for the determination of the resulting drug concentration-position profiles within the mini-matrices as a function of time and confirmed the theoretical predictions.

1. Introduction

Incorporation of a drug within a polymeric matrix is often used to control the resulting drug release kinetics [1–4]. To produce such advanced drug delivery systems, hot-melt extrusion is becoming a widely used technology in the pharmaceutical industry [5–7]. The group of James McGinity made major contributions to this highly promising field e.g. [8–10]. Importantly, a variety of thermoplastic polymers can serve as matrix formers in this type of dosage forms and very different release patterns can be provided [11–13]. For instance, it has recently been shown that cylindrical mini-matrices (prepared by hot-melt extrusion) allow for a broad variety of release rates when using ethylcellulose as a matrix former. The addition of different amounts of release rate modifiers, such as hydroxypropyl methylcellulose [14–16], xanthan gum [17,18] or polyethylene glycol/polyethylene oxide [19], presents an efficient tool to adjust the desired drug release patterns. For example, increasing amounts of xanthan gum in the matrices lead to significant system swelling upon contact with aqueous fluids and, thus, accelerated drug release [17,18]. Interestingly, also the average molecular weight of the polymer of the release rate modifier can significantly affect the resulting drug release profiles [19].

Despite the steadily increasing practical importance of this type of advanced drug delivery systems, very little is known on the mechanisms controlling drug release from these dosage forms [20]. Thus, there is a significant lack of appropriate mathematical models allowing for facilitated device optimization [21]. Generally, the systems are treated as "black boxes", and time-consuming and cost-intensive series of trial-and-error experiments are required to optimize them. Often, diffusional mass transport plays a major role in the control of drug release from polymeric devices [22,23]. In these cases, it is decisive to consider the three-dimensional geometry of the systems. If the latter are cylindrical in shape, diffusional mass transport in axial as well as in radial direction should be taken into account [24,25]. Furthermore, great care must be

* Corresponding author. Laboratory of Pharmaceutical Technology, Ghent University, Harelbekestraat 72, 9000 Gent, Belgium. Tel.: +32 9 2648069; fax: +32 9 2228236.
E-mail address: Chris.Vervaet@UGent.be (C. Vervaet).

0939-6411/$ - see front matter © 2009 Elsevier B.V. All rights reserved.
doi:10.1016/j.ejpb.2009.06.010

paid with respect to potential time- and position-dependencies of the diffusivities of the involved species [26]. If for instance, the conditions for drug diffusion significantly change with time within the dosage form (e.g. due to dynamic changes in the matrix porosity), this phenomenon must be taken into account in the mathematical theory. Importantly, an appropriate mathematical model not only allows for the determination of system-specific parameters and, thus, for a better understanding of the underlying drug release mechanisms, but also allows the mechanistic realistic theory for the prediction of the effects of formulation and processing parameters on the resulting drug release kinetics in a quantitative way. Hence, the development of novel devices of this type or the optimization of the existing ones can be significantly facilitated [27]. The validity of such advanced mathematical theories should be evaluated by the comparison of theoretical predictions and independent experimental measurements. This should include the prediction of the resulting drug release kinetics (as a function of design parameters) and – if possible – also of other types of system characteristics, e.g. dynamic changes in the drug concentration-position profiles within the matrices. The latter might experimentally be determined using advanced characterization techniques such as Raman spectroscopy.

The major aims of the present study were (i) to better understand the underlying drug release mechanisms in hot-melt extruded mini-matrices, (ii) to identify/develop appropriate, mechanistic realistic mathematical theories allowing for quantitative predictions of the effects of formulation variables on the resulting drug release profiles, and (iii) to evaluate the validity of these theories using independent experimental measurements. Metoprolol tartrate was selected as a model drug, ethylcellulose as a matrix former and polyethylene glycol (PEG)/polyethylene oxide (PEO) as a release rate modifier.

2. Materials and methods

2.1. Materials

Metoprolol tartrate (10 μm) (Esteve Quimica, Barcelona, Spain) was selected as a model drug. The matrix consisted of ethylcellulose (Ethocel® Std 10 FP Premium, particle size: 3–15 μm), kindly donated by Dow Chemical Company (Midland, USA), and a hydrophilic component: polyethylene glycol (PEG 6000) (Fagron, Waregem, Belgium) or polyethylene oxide (PEO, Sentry™ Polyox™ WSR N10, N12 K and 303, molecular weight (MW): 100,000, 1,000,000 and 7,000,000, respectively) (Dow Chemical Company, Midland, USA). Dibutyl sebacate (DBS) (Sigma–Aldrich, Steinheim, Germany) was used as a plasticizer for ethylcellulose. All other chemicals were of analytical grade.

2.2. Preparation of mini-matrices via hot-melt extrusion

The composition of the investigated mini-matrices is shown in Table 1. For all formulations, the metoprolol tartrate content was kept constant at 30% (w/w), while the concentration of the hydrophilic polymer (PEG or PEO) was varied between 0% and 20% (w/w). The remaining part of the formulation consisted of ethylcellulose/DBS, blended at a ratio of 2/1 (w/w) [18].

Table 1
Composition (%, w/w) of the investigated mini-matrices.

Metoprolol tartrate	30	30	30	30	30	30
PEG/PEO	–	1	2.5	5	10	20
Ethylcellulose	46.7	46	45	43.3	40	33.3
DBS	23.3	23	22.5	21.7	20	16.7

The components were blended in a planetary mixer (15 min, 90 rpm) (Kenwood Major Classic, Hampshire, UK) and incubated overnight at room temperature to allow for interaction between ethylcellulose and the plasticizer. The mixture was passed through the screws of the powder feeder of a MP19TC-25 extruder (APV Baker, Newcastle-under-Lyme, UK) at room temperature and recycled into the powder reservoir prior to hot-melt extrusion to assure blend homogeneity. Hot-melt extrusion was performed using a laboratory-scale intermeshing co-rotating twin-screw extruder (MP19TC-25) with a length-to-diameter ratio of 25/1. The machine was equipped with a Brabender twin-screw powder feeder, a screw with two mixing sections and a densification zone [18]. The die block (2.6 cm thickness) was fixed to the extruder barrel and the axially mounted die plate (1.9 cm thickness, with a cylindrical hole of 3 mm diameter for shaping the extrudates) was attached to the die block. The following extrusion conditions were used: screw speed = 30 rpm, powder feed rate = 6 g/min, temperature = 40 and 70 °C in the five heating zones along the barrel for extrusion of PEG- and PEO-containing formulations, respectively. After cooling down to room temperature, the extruded rods were manually cut into mini-matrices of desired length using surgical blades. Dies with different dimensions (varying between 1 and 12 mm) were used in order to produce extrudates of different diameters.

2.3. In vitro drug and PEG/PEO release

Metoprolol tartrate release from the mini-matrices (approximately 60 mg) was determined using the USP apparatus 1 (rotating basket, 100 rpm, 4 mini-matrices per vessel) (VK 7010, combined with a VK 8000 automatic sampling station, VanKel, New Jersey, USA). Demineralised water (900 mL, 37 ± 0.5 °C) was used as release medium (solubility of metoprolol tartrate > 1 g/ml). At predetermined time points, 5-mL samples were withdrawn and analyzed for the drug content by UV spectroscopy (λ = 222 nm, Lambda 12 UV–Vis double-beam spectrophotometer, Perkin Elmer, Zaventem, Belgium). Each experiment was conducted six times.

PEG/PEO release from the mini-matrices was determined using the USP paddle method under the same conditions as described above. PEG/PEO concentrations in the samples were measured by gel filtration chromatography (GFC) (detection via changes in the refractive index) [19]. Briefly, for PEG 6000 and PEO 100,000 analysis, a Waters 600 Controller/Waters 610 Fluid Unit pump (flow rate: 1.0 mL/min) with a Waters 410 Differential Refractometer was used. A 20-μL sample (using a 100 μL Hamilton syringe) was injected into the column (TSK-gel® G 4000 PW (TosoHaas; 7.5 mm ID × 30 cm – particle size 17 μm) and TSK-gel® G 3000 PW (7.5 mm ID × 30 cm – particle size 10 μm) coupled in series). PEO 1,000,000 and 7,000,000 samples were analyzed using a Waters 515 HPLC pump (flow: 1.0 mL/min) combined with a Waters Differential Refractometer R401. A 20-μL sample was injected into the column (TSK-gel® G 6000 PW (7.5 mm ID × 30 cm – particle size 17 μm) and TSK-gel® G 5000 PW (7.5 mm ID × 30 cm – particle size 10 μm) coupled in series). The chromatograms were integrated using the Millennium 2010 Chromatography Manager (Version 2.15.01). The mobile phase consisted of water (Milli-Q® Water Purification System), filtered using Durapore® membrane filters (0.45 μm – HVLP type) and degassed with helium. Due to the sensitivity of the GFC analysis, the sample size was adapted (36, 9 and 5 g mini-matrices for the 2.5%, 10% and 20% PEG/PEO formulations, respectively). All experiments were conducted in duplicate.

In case drug or PEG/PEO release levelled off below 100%, the experimentally determined plateau value was considered as the 100% reference value for the modeling of drug and PEG/PEO release (=amounts of mobile species).

2.4. Porosity of the mini-matrices

To determine dynamic changes in the porosity of the mini-matrices upon exposure to the release medium, 40 mini-matrices were subjected to the same conditions as described above for the in vitro release studies. At predetermined time points, the mini-matrices were withdrawn, deep-frozen using liquid nitrogen and freeze-dried (Amsco-Finn Aqua GT4 freeze-dryer, Amsco, Darmstadt, Germany). The mini-matrices were stored over silica prior to true volume measurements with a helium pycnometer (AccuPyc 1330, Micromeritics, Norcross, USA). The porosity of the mini-matrices was calculated based on these values and on the mini-matrices' apparent volume, which was determined using a digital calliper (Bodson, Luik, Belgium).

2.5. X-ray tomography

The mini-matrices (before exposure to the release medium, and after 24 h exposure to the release medium) were scanned with the in-house developed high-resolution micro-CT scanner of the Ghent University Centre for X-ray Tomography (www.UGCT.ugent.be). The system is composed of a Feinfocus X-ray tube with transmission target and beryllium exit window, a Micos high precision air-bearing rotation stage and a Varian Paxscan 2520 a-Si flat panel detector. The tube was operated at 60 kV tube voltage in micro-focus mode at 2.8 W, which results in a 3 μm spot size. During scanning, the sample was rotated over 360° in 0.45° steps where four shadow images were recorded in every step. The detector consists of a CsI screen with 2000 × 1600 pixels of 127 μm and it was operated in non-binning mode with an exposure time of 2 s. The source-to-object distance was kept at 20 mm and the source-to-detector distance was at 860 mm in order to have a factor 42 magnification with 3 μm resolution.

The 800 shadow images were processed and reconstructed to 1500 cross-sectional images of 1100 × 1100 pixels with 3 μm pixel size with Octopus software. From each mini-matrix, a central region of 300 slices was used for statistical analysis.

To process the images, two selections were made: one with the material of the mini-matrix and another one with the pores. This was achieved by segmentation based on the greyscale, and subsequent filtering to remove the noise (these results should be sceptically analyzed as limiting factors such as noise and resolution make the obtaining of these results slightly operator dependent). The voids were subsequently separated and classified for equivalent diameters. Separating the pores makes it possible to have a better analysis of the porosity but it removes the pore interconnectivity; however, the pores are mostly connected through ducts with a diameter of about 1 μm and the resolution of the scan is not sufficient to analyze this. Equivalent diameters means that for each pore the volume was calculated in μm^3 and that volume is then considered as a perfect sphere, the diameter of this calculated sphere is the equivalent diameter.

The set of 300 cross-sections statistically analyzed were subsequently loaded in a three-dimensional rendering software (VGstudio). In this way, it is made possible to represent the porosity and the size distribution of the pores.

2.6. Raman analysis

MPT distribution in the mini-matrices, before exposure to the dissolution medium and 24 h after exposure to the release medium, was evaluated by Raman spectroscopic mapping. Prior to Raman analysis, the tablets obtained after 24 h of dissolution were frozen using liquid nitrogen and freeze-dried over 25 h, as described above to determine the porosity. After freeze-drying, the samples were cut along their radial (Fig. 1a) and axial axes

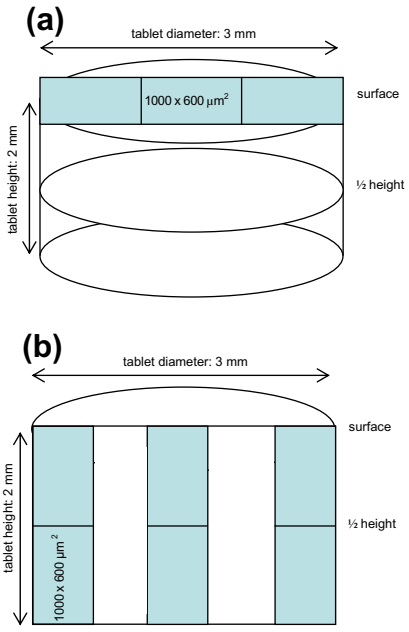

Fig. 1. Schematic drawing of the areas (presented as blue rectangles) mapped with Raman spectroscopy: (a) surface and half height (radial cutting surface) are mapped along the diameter of the mini-matrix and (b) six areas of the axial cutting surface are mapped. (For interpretation of the references to colour in this figure legend, the reader is referred to the web version of this article.).

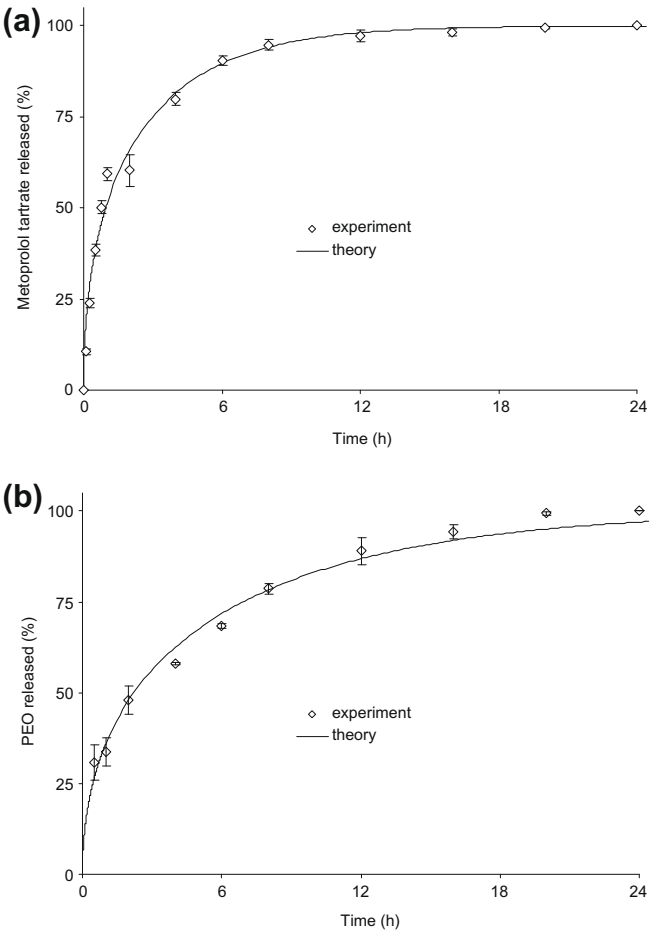

Fig. 2. Experiment (symbols) and theory (curves, "simple" model assuming constant diffusion coefficients, Eq. (2)): (a) metoprolol tartrate release from mini-matrices initially containing 20% PEO 1000,000 and (b) PEO release from mini-matrices initially containing 10% PEO 100,000.

(Fig. 1b). At the exterior surface as well as at the radial cutting surface, three areas (1000 × 600 μm², Fig. 1a) (n = 3) were scanned using a 10×-long working distance objective lens (laser spot size: 50 μm) in point-by-point mapping mode with a step size of 50 μm in both the x and y directions. In addition, 24 h after exposure to the release medium, six areas (1000 μm × 600 μm, Fig. 1b) (n = 3) of the axial cutting surface were mapped via Raman spectroscopy.

The resulting map provides an overview of the MPT distribution in the mapped area. The mapping system used for this study was a RamanRxn 1 Analyzer and Microprobe (Kaiser Optical Systems, Ann Arbor, USA), equipped with an air-cooled CCD detector (back-illuminated deep depletion design). The laser wavelength during the experiments was the 785 nm line from a 785 nm Invictus NIR diode laser. All spectra were recorded at a resolution of 4 cm^{-1} using a laser power of 400 mW and a laser light exposure time of 30 s per collected spectrum. Before data analysis, spectra were baseline corrected. Data collection and data analysis were done using the HoloGRAMS™ data collection software package, the HoloMAP™ data analysis software and Matlab® software package (version 6.5.).

3. Results and discussion

Previous work of the authors has shown that the release rates of metoprolol tartrate (used as model drug) and PEG/PEO from hot-melt extruded mini-matrices strongly depend on the concentration as well as on the type of PEG/PEO incorporated in the ethylcellulose-based cylinders [19]. The aim of this study was to better understand the underlying mass transport mechanisms in these systems and to be able to quantitatively predict the effects of the device design on the resulting drug release kinetics.

3.1. "Simple" mathematical theory

As diffusion is likely to play a major role in the control of drug and PEG/PEO release, Fick's second law was used as a basis for the mathematical analysis. Importantly, the cylindrical geometry of the mini-matrices was taken into account and radial as well as axial mass transport was considered [28]:

$$\frac{\partial c_k}{\partial t} = \frac{1}{r}\left\{\frac{\partial}{\partial r}\left(rD_k\frac{\partial c_k}{\partial r}\right) + \frac{\partial}{\partial \theta}\left(\frac{D_k}{r}\frac{\partial c_k}{\partial \theta}\right) + \frac{\partial}{\partial z}\left(rD_k\frac{\partial c_k}{\partial z}\right)\right\} \quad (1)$$

where c_k and D_k are the concentration and diffusion coefficients of the diffusing species (k = 1: drug; k = 2: PEG/PEO), respectively; t represents time; and r, z and θ denote the radial, axial and angular coordinates, respectively. This partial differential equation was solved considering the following initial and boundary conditions:

- The drug and PEG/PEO are initially homogeneously distributed throughout the mini-matrices (before exposure to the release medium, t = 0).
- Perfect sink conditions are maintained throughout the experiments for all diffusing species.
- The cylinders do not significantly swell or shrink during drug release.
- The diffusion coefficients of metoprolol tartrate and PEG/PEO are constant during the entire drug release period.

Using the method of Laplace transform, the following analytical solution of Fick's law can be derived [29]:

Table 2
The effects of the initial PEG/PEO concentrations and molecular weights (MW) on the apparent diffusion coefficient of metoprolol tartrate (D_{drug}) and PEG/PEO ($D_{PEG/PEO}$) determined with the "simple" mathematical model in the investigated mini-matrices (mean ± SD, n = 6).

PEG/PEO concentration (%, w/w)	MW PEG/PEO (Da)	D_{drug} (cm^2/s)	$D_{PEG/PEO}$ (cm^2/s)
0	–	Non-constant	–
1	6000	–	–
	100,000	–	–
	1,000,000	–	–
	7,000,000	Non-constant	–
2.5	6000	–	$4.2\ (\pm0.4) \times 10^{-8}$
	100,000	$1.9\ (\pm0.0) \times 10^{-8}$	Non-constant
	1,000,000	–	Non-constant
	7,000,000	Non-constant	Non-constant
5	6000	$2.3\ (\pm0.3) \times 10^{-8}$	–
	100,000	$2.2\ (\pm0.2) \times 10^{-8}$	–
	1,000,000	Non-constant	–
	7,000,000	Non-constant	–
10	6000	$2.6\ (\pm0.2) \times 10^{-8}$	$1.2\ (\pm0.0) \times 10^{-7}$
	100,000	$2.5\ (\pm0.2) \times 10^{-8}$	$6.7\ (\pm0.7) \times 10^{-8}$
	1,000,000	Non-constant	$6.2\ (\pm1.5) \times 10^{-8}$
	7,000,000	Non-constant	Non-constant
20	100,000	$4.5\ (\pm0.9) \times 10^{-7}$	$1.4\ (\pm0.2) \times 10^{-7}$
	1000,000	$1.6\ (\pm0.8) \times 10^{-7}$	$7.1\ (\pm1.3) \times 10^{-8}$
	7,000,000	$2.0\ (\pm0.2) \times 10^{-7}$	$7.3\ (\pm0.1) \times 10^{-8}$

–: Not determined.

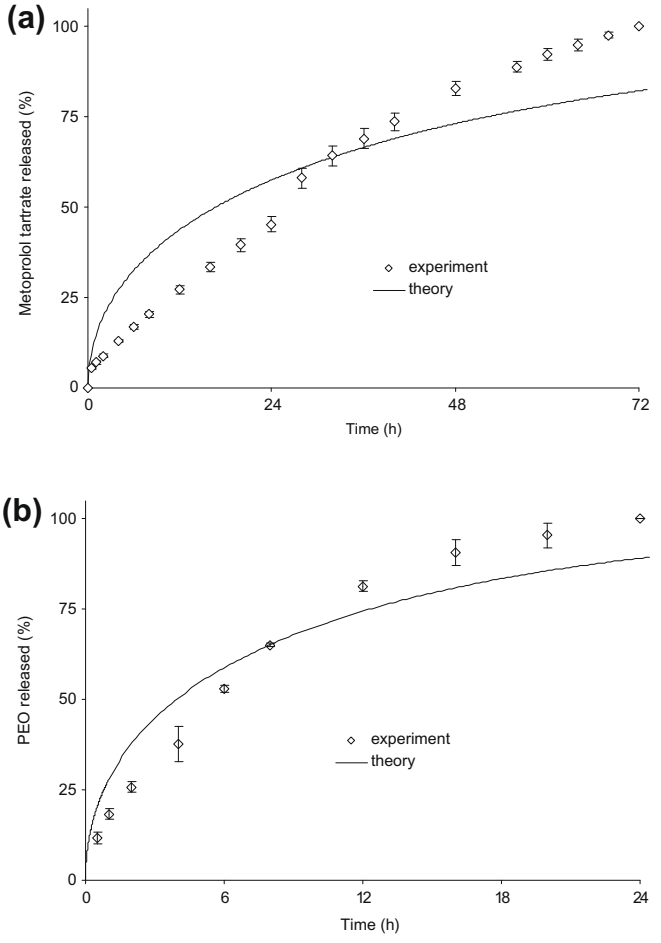

Fig. 3. Experiment (symbols) and theory (curves, "simple" model assuming constant diffusion coefficients, Eq. (2)): (a) metoprolol tartrate release from mini-matrices free of PEG/PEO and (b) PEO release from mini-matrices initially containing 10% PEO 7000,000.

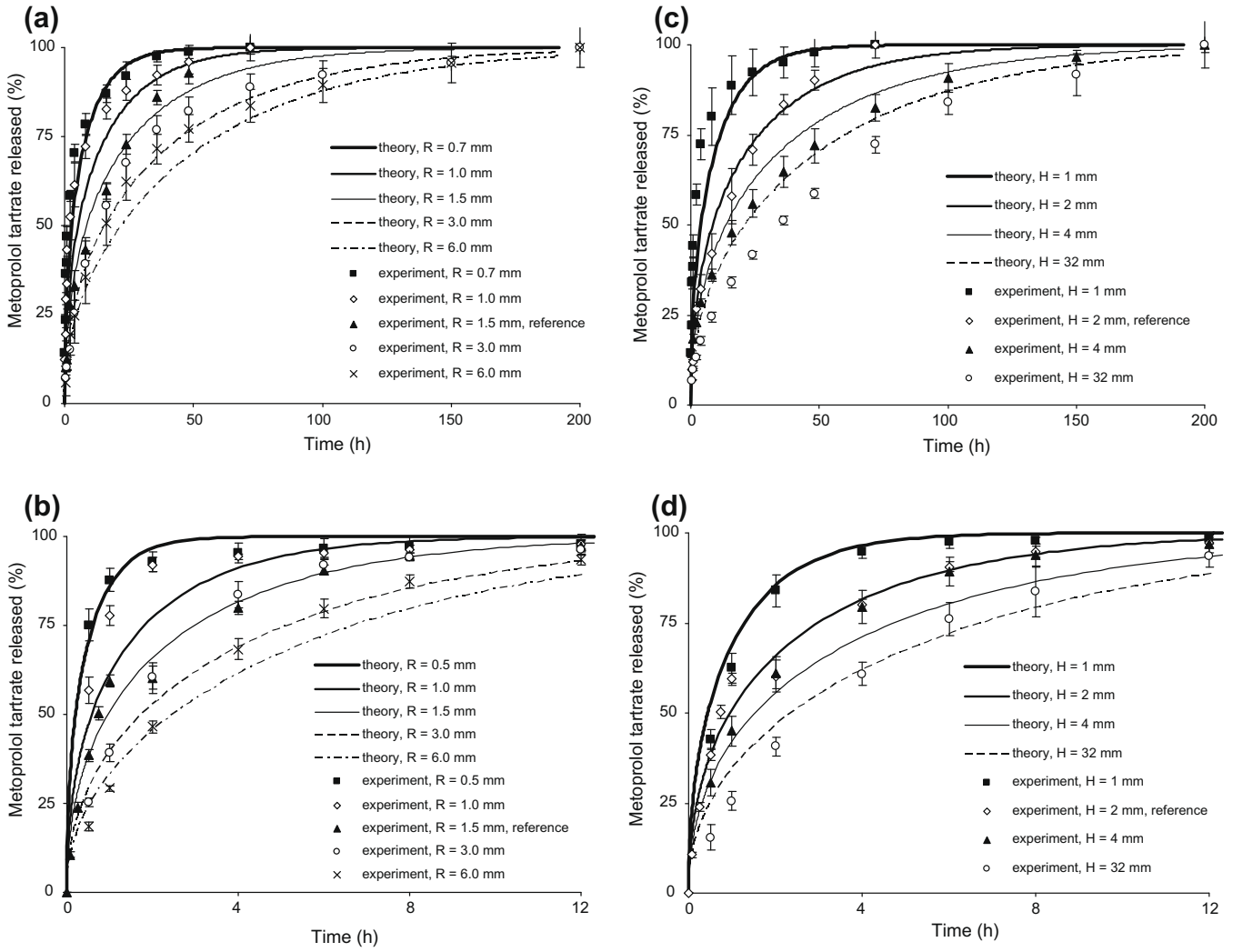

Fig. 4. Theoretical predictions and independent experimental verification (except for the reference formulations) of the effects of the cylinders' radii and heights (indicated in the figures) on the resulting metoprolol tartrate release kinetics from mini-matrices initially containing: (a) 10% PEO 100,000 (constant height = 2 mm), (b) 20% PEO 1,000,000 (constant height = 2 mm), (c) 10% PEO 100,000 (constant radius = 1.5 mm), and (d) 20% PEO 1,000,000 (constant radius = 1.5 mm).

$$\frac{M_{k,t}}{M_{k,\infty}} = 1 - \frac{32}{\pi^2} \cdot \sum_{n=1}^{\infty} \frac{1}{q_n^2} \cdot exp\left(-\frac{q_n^2}{R^2} \cdot D_k \cdot t\right) \cdot \sum_{p=0}^{\infty} \frac{1}{(2p+1)^2} \cdot exp\left(-\frac{(2p+1)^2 \cdot \pi^2}{H^2} \cdot D_k \cdot t\right) \quad (2)$$

where $M_{k,t}$ and $M_{k,\infty}$ are the amounts of drug or PEG/PEO released at time t and at infinite time ($k = 1$: drug; $k = 2$: PEG/PEO), respectively; the q_n are the roots of the Bessel function of the first kind of order zero [$J_0(q_n) = 0$]; R and H represent the radius and height of the cylinder; D_k denotes the constant diffusion coefficient of the drug or PEG/PEO.

Eq. (2) was fitted to the experimentally measured drug and PEG/PEO release profiles (using Mathematica 7) from the investigated ethylcellulose-based mini-matrices containing 0–20% (w/w) PEG/PEO of different molecular weights (6000–7,000,000 Da). Examples for such fittings are shown in Fig. 2. As it can be seen, good agreement between theory and experiment was obtained in the case of metoprolol tartrate and PEO release from cylinders initially containing 20% PEO 1,000,000 and 10% PEO 100,000, respectively. This indicates that the mass transport of both species is likely to be dominated by pure diffusion with constant diffusion coefficients. Based on these fittings, the apparent diffusivities of metoprolol tartrate and PEO in these systems could be determined to be equal to 1.6 (±0.8) × 10^{-7} cm^2/s and 6.7 (±0.7) × 10^{-8} cm^2/s, respectively. In Table 2, the diffusion coefficients of the respective species in the various investigated mini-matrices are shown. However, significant deviations were also observed between the theoretically calculated drug and the excipient release profiles and the experimentally measured ones. Fig. 3 shows two examples: drug and PEO release from mini-matrices initially free of PEG/PEO and from mini-matrices initially containing 10% PEO 7,000,000, respectively. Thus, in these cases, the underlying mass transport mechanisms are more complex. Table 2 gives an overview on the investigated systems, indicating whether the "simple" mathematical model considering constant diffusion coefficients (Eq. (2)) was appropriate (either D values are indicated, or "non-constant" is marked). Importantly, there is a clear tendency: drug and PEG/PEO release predominantly controlled by pure diffusion with constant diffusion coefficients: (i) at high initial PEG/PEO loadings (≈20%), irrespective of the molecular weight of the PEG/PEO and (ii) at intermediate PEG/PEO loadings (2.5–10%) in the case of low molecular weight PEG/PEOs MW ⩽ 100,000 Da). In these cases, the leaching of the water-soluble excipients is relatively rapid, and time-dependent changes in the matrix porosity are only of minor importance for diffusional mass transfer to occur.

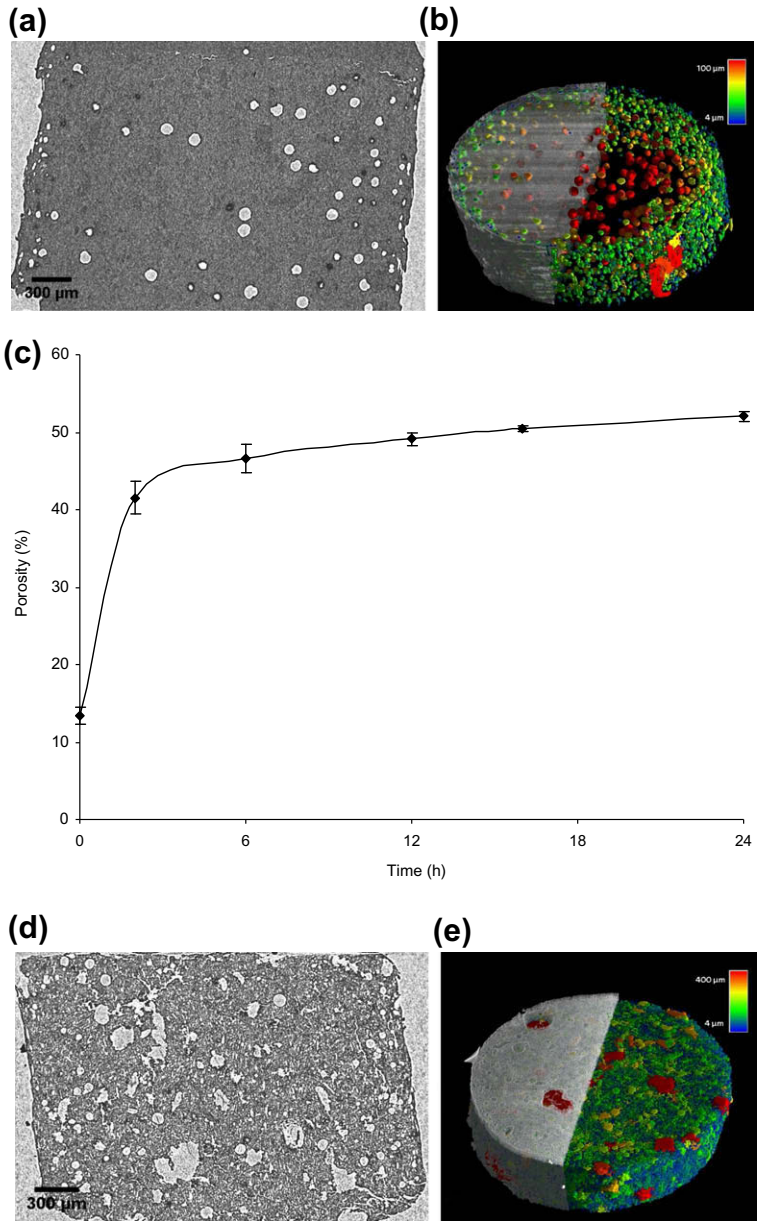

Fig. 5. Porosity of mini-matrices initially containing 10% PEO 7,000,000 before and after exposure to the release medium: (a) cross-section at $t = 0$ h (before exposure), (b) visualization of the pores using X-ray tomography at $t = 0$ h (before exposure), (c) time-dependent increase in porosity measured using a helium pycnometer, (d) cross-section after 24 h exposure, and (e) visualization of the pores using X-ray tomography after 24 h exposure.

In contrast, at low initial PEG/PEO loadings and at intermediate PEG/PEO loadings of high molecular weight PEG/PEOs, the mobility of incorporated molecules is likely to be affected by the dynamic changes in the matrix porosity: with increasing pore size, the mobility of the drug and water-soluble excipients significantly increases. This hypothesis is in good agreement with the type of systematic deviations observed between the fitted theory (“simple” model assuming time-independent, “average” diffusivities) and the experimentally determined amounts of released metoprolol tartrate and PEG/PEO (Fig. 3): at early time points, diffusional mass transport is theoretically overestimated (due to the lower real mobility), whereas at late time points, it is underestimated (due to the higher real mobility).

In addition to this deeper insight into the underlying mass transport mechanisms, the mathematical modeling of the mini-matrices, which can be described by Eq. (2) (“simple” theory), also offers an interesting practical benefit: the effects of the initial radius and height of the cylinders on the resulting drug and PEG/PEO release kinetics can be predicted in a quantitative way. Fig. 4 shows some examples for such predictions. Knowing the diffusion coefficients of metoprolol tartrate and PEG/PEO from the fittings of the “simple” model to the release kinetics from mini-matrices initially containing 10% or 20% (w/w) PEO with a height of 2 mm and a radius of 1.5 mm, drug leaching into the release medium was predicted from cylinders with the same radius, but varying thickness (curves in Fig. 4a and b), or with the same height, but varying radius (curves in Fig. 4c and d). As it can be seen in Fig. 4a and b, a significant decrease in the relative mass transport rates was predicted with increasing radius of the cylinders. This is due to the increase in the length of the diffusion pathways. Importantly, these theoretical predictions (curves) could be confirmed by independent experimental metoprolol tartrate leaching measurements (symbols in Fig. 4a and b). This clearly indicates that drug release from these hot-melt extruded mini-matrices is predominantly

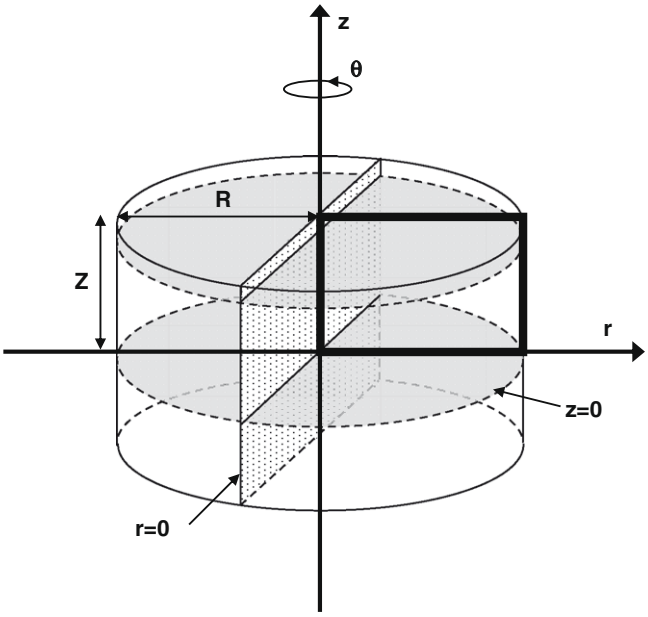

Fig. 6. Schematic presentation of a cylindrical mini-matrix for the mathematical analysis with the "complex" model. The symmetry planes for $r = 0$ and $z = 0$ as well as the rotational symmetry of the system with respect to the angle θ are indicated. Furthermore, the location of the cross-section referred to in Fig. 9 is illustrated.

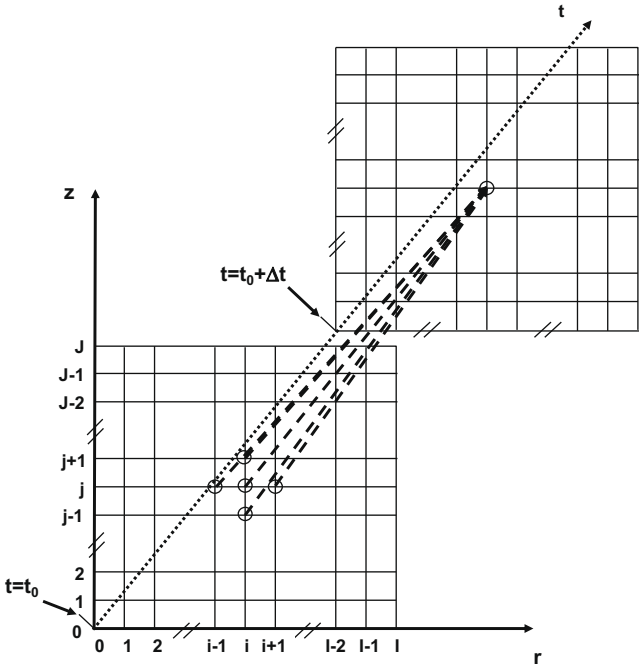

Fig. 7. Schematic presentation of the basic principle of the applied numerical analysis for the "complex" mathematical model considering time-dependent diffusion coefficients.

controlled by pure diffusion with constant diffusion coefficients. The theoretically predicted effects of the height of mini-matrices initially containing 10% PEO 100,000 or 20% PEO 1,000,000 on the resulting drug release kinetics from cylinders with a constant radius of 2 mm are illustrated in Fig. 4c and d (curves). Clearly, the variation of the cylinder height from 1 to 32 mm strongly affected the resulting drug release patterns. Again, an increase in the length of the diffusion pathways led to decreasing relative metoprolol tartrate release rates. Compared to the effects of the cylinder radius, the consequences of the relative changes in the matrix height are less pronounced. This can be attributed to the fact that the surface area of a cylinder depends on the radius to the power of two and to the height to the power of one only. Importantly, also in these cases, independent metoprolol tartrate release measurements confirmed the theoretical predictions (symbols in Fig. 4c and d).

3.2. "Complex" mathematical theory

To better understand the observed systematic deviations between the "simple" mathematical theory and the experimentally determined drug and PEG/PEO release kinetics from mini-matrices with low initial PEG/PEO loadings and with intermediate initial PEG/PEO loadings of high molecular weight, the porosity of the mini-matrices was determined before and upon exposure to the release medium using X-ray tomography as well as a helium pycnometer. As it can be seen in Fig. 5a–c, the mini-matrices already showed an initial porosity at the beginning (before exposure to the release medium, at $t = 0$). Importantly, this porosity significantly increased upon exposure to the release medium (Fig. 5c), at least partially due to drug and PEG/PEO leaching into the bulk fluid. After 24 h exposure, highly porous matrices were observed, which also partially showed crack formation (Fig. 5d and e).

This significant increase in the matrix porosity is not taken into account by the "simple" mathematical theory. The time-dependent changes in the system porosity are likely to result in significant changes in the mobility of the drug and PEG/PEO, especially at low initial PEG/PEO loadings (due to the limited pore volume available for diffusion). It has to be pointed out that drug and PEG/PEO diffusion through the ethylcellulose (even plasticized) is much slower than drug and PEG/PEO diffusion through water-filled pores. The following, more complex mathematical theory takes the time-dependent drug and PEG/PEO mobility quantitatively into account. It is also based on Fick's law of diffusion, considering radial and axial mass transport in cylinders (Eq. (1)) (Fig. 6). The underlying model assumptions are as follows:

- The drug and PEG/PEO are initially homogeneously distributed throughout the mini-matrices (before exposure to the release medium, $t = 0$).
- Perfect sink conditions are maintained throughout the experiments for all diffusing species.
- The cylinders do not significantly swell or shrink during drug and PEG/PEO release.

As time-dependent drug and PEG/PEO diffusion coefficients are taken into account, there is no analytical solution for this initial value problem. Thus, a numerical method, based on finite differences was applied. In the following, only a brief description is given, and the reader is referred to the literature for details [29,30]. As there is no concentration gradient of any component with respect to the angle θ (Fig. 6), Eq. (1) can be transformed into:

$$\frac{\partial c_k}{\partial t} = \frac{\partial}{\partial r}\left(D_k \frac{\partial c_k}{\partial r}\right) + \frac{D_k}{r}\frac{\partial c_k}{\partial r} + \frac{\partial}{\partial z}\left(D_k \frac{\partial c_k}{\partial z}\right) \quad (3)$$

To minimize the computation time, the symmetry plane at $z = 0$ (Fig. 6) is also taken into account. Thus, it is sufficient to describe the changes in the metoprolol tartrate and PEG/PEO concentrations within the two-dimensional rectangle highlighted in Fig. 6 to be able to calculate the mass transport phenomena in the entire cylinder: upon rotation around the z-axis, the upper half of the mini-matrix is described, and due to the symmetry at $z = 0$ plane, the whole cylinder can be considered. The initial condition takes into account that metoprolol tartrate as well as PEG/PEO is uniformly distributed throughout the mini-matrices before exposure to the release medium (at $t = 0$). Thus, the drug and PEG/PEO

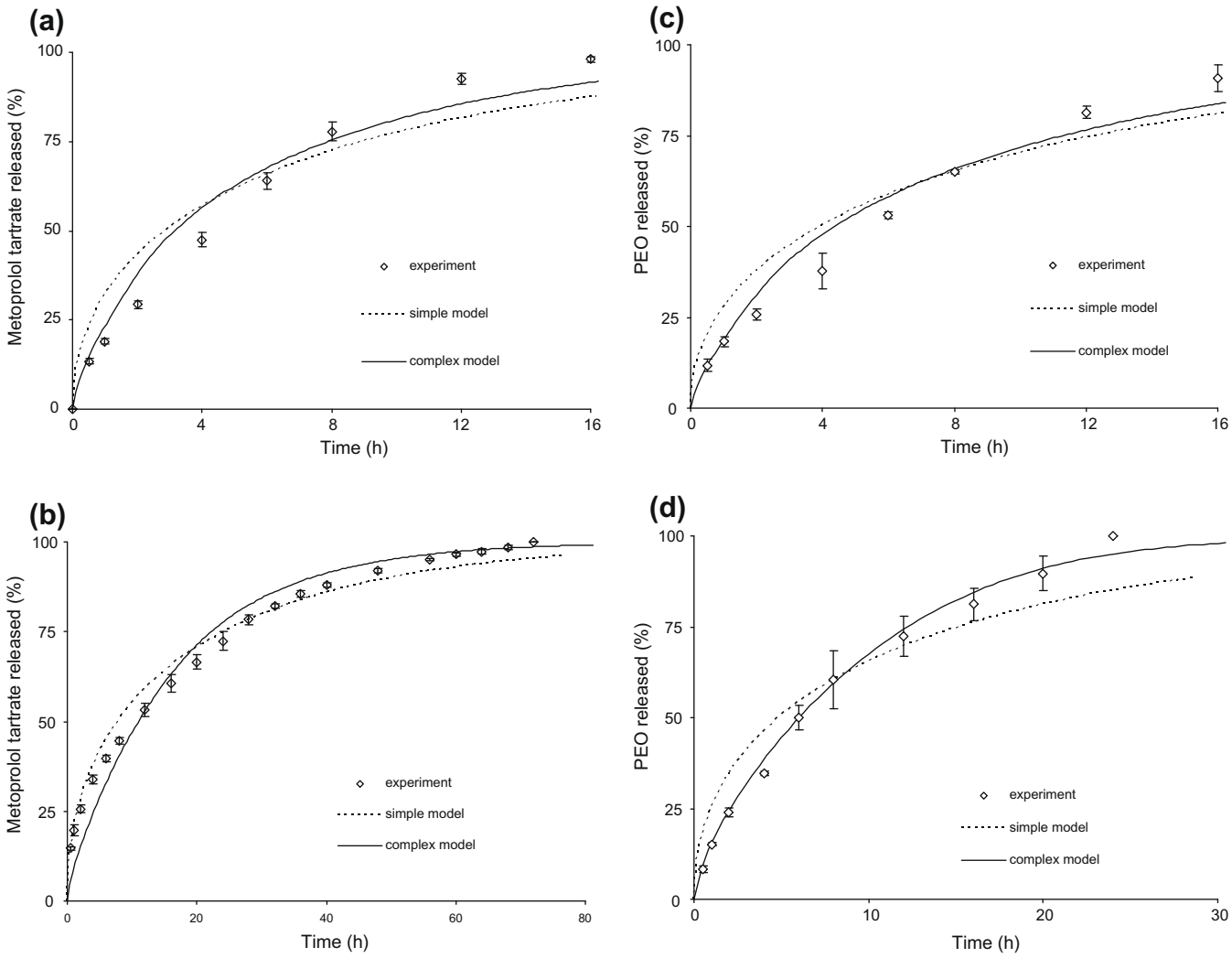

Fig. 8. Experiment (symbols) and theory (dashed curves: "simple" model assuming constant diffusion coefficients, solid curves: "complex" model considering time-dependent diffusion coefficients): (a) metoprolol tartrate release from mini-matrices initially containing 10% PEO 7,000,000, (b) metoprolol tartrate release from mini-matrices initially containing 2.5% PEO 100,000, (c) PEO release from mini-matrices initially containing 10% PEO 7,000,000, and (d) PEO release from mini-matrices initially containing 2.5% PEO 100,000.

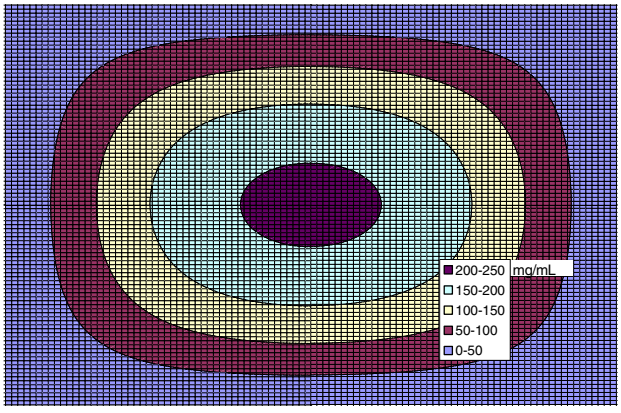

Fig. 9. Theoretical prediction ("complex" model) of the metoprolol tartrate concentration-position profile within mini-matrices initially containing 2.5% PEO 100,000 after 24 h exposure to the release medium: cross-section at $r = 0$ (see Fig. 6).

concentrations at any position are equal to the respective initial concentrations ($c_{1\ initial}$, $c_{2\ initial}$):

$$t = 0 \quad C_1 = C_{1\ initial} \quad 0 \le r \le R \quad 0 \le z \le Z \tag{4}$$

$$t = 0 \quad C_2 = C_{2\ initial} \quad 0 \le r \le R \quad 0 \le z \le Z \tag{5}$$

where R denotes the radius and Z the half height of the mini-matrix. As perfect sink conditions are provided for all diffusing species throughout the experiments, the metoprolol tartrate and PEG/PEO concentrations at the surface of the cylinders are always maintained at zero upon exposure to the release medium:

$$t > 0 \quad C_1 = 0 \quad 0 \le r \le R \quad z = Z \tag{6}$$

$$t > 0 \quad C_1 = 0 \quad 0 \le z \le Z \quad r = R \tag{7}$$

$$t > 0 \quad C_2 = 0 \quad 0 \le r \le R \quad z = Z \tag{8}$$

$$t > 0 \quad C_2 = 0 \quad 0 \le z \le Z \quad r = R \tag{9}$$

Due to the symmetries at the planes at $z = 0$ and $r = 0$ (Fig. 6), there are no concentration gradients at $z = 0$ for $0 \leqslant r \leqslant R$ and at $r = 0$ for $0 \leqslant z \leqslant Z$ for any of the diffusing components:

$$t > 0 \quad \frac{\partial C_1}{\partial z} = 0 \quad 0 \le r \le R \quad z = 0 \tag{10}$$

$$t > 0 \quad \frac{\partial C_1}{\partial r} = 0 \quad 0 \le z \le Z \quad r = 0 \tag{11}$$

$$t > 0 \quad \frac{\partial C_2}{\partial z} = 0 \quad 0 \le r \le R \quad z = 0 \tag{12}$$

$$t > 0 \quad \frac{\partial C_2}{\partial r} = 0 \quad 0 \le z \le Z \quad r = 0 \tag{13}$$

Furthermore, the time-dependent porosity of the matrices is taken into account (Fig. 5c). The increase in metoprolol tartrate and PEG/PEO mobility within the mini-matrices as a function of the system porosity is considered as follows:

$$D_k(t) = \frac{D_{k\ crit} \cdot \varepsilon(t)}{100} \tag{14}$$

where $D_{k\ crit}$ represents a critical diffusion coefficient of the drug and PEG/PEO (as diffusion takes place in confined regions, this value is not necessarily equal to the diffusivity in pure water) and ε denotes the porosity of the cylinder in percent. Thus, the consequences of the dynamic changes in the structure of the mini-matrices during drug release for the multi-component diffusion are quantitatively taken into account.

To calculate the changes in the metoprolol tartrate and PEG/PEO concentrations within the two-dimensional rectangle highlighted in Fig. 6, the radius of the mini-matrix, R, and half height, Z, are divided into I and J space intervals, Δr and Δz, respectively (Fig. 7). This generates a grid of $(I+1) \times (J+1)$ grid points. The time is divided into g time intervals Δt. At $t = 0$ (before exposure to the release medium), the drug and PEG/PEO concentrations are known from the initial conditions (Eqs. (4),(5)). Using Eqs. (3), (6)–(13), (and) (14), the concentration profiles of the diffusing species at a new time step ($t = t_0 + \Delta t$) can be calculated, when the concentration profiles are known at the previous time step ($t = t_0$): the concentration of the drug and PEG/PEO at a certain inner grid point ($i \times \Delta r$, $j \times \Delta z$) at the new time step ($t = t_0 + \Delta t$) is calculated from its concentrations at the same grid point ($i \times \Delta r$, $j \times \Delta z$) and the four direct neighbors [$(i-1) \times \Delta r$, $j \times \Delta z$; $i \times \Delta r$, $(j-1) \times \Delta z$; $i \times \Delta r$, $(j+1) \times \Delta z$; $(i+1) \times \Delta r$, $j \times \Delta z$] at the previous time step ($t = t_0$) (Fig. 7). The respective concentrations at the outer grid points ($i = 0$, $i = I$, $j = 0$, $j = J$) at a new time step ($t = t_0 + \Delta t$) are calculated using the boundary conditions (Eqs. (6)–(13)). As all initial concentrations are known, the concentration profiles at $t = 0 + \Delta t$, $t = 0 + 2\Delta t$, $t = 0 + 3\Delta t$,..., $t = 0 + g\Delta t$ can be calculated sequentially. Furthermore, the total amounts of metoprolol tartrate and PEG/PEO within the cylinders are calculated at each time step (by integrating the respective concentrations with respect to r, z and θ). Based on the experimentally determined porosity of the mini-matrices, the drug and PEG/PEO diffusivities can be calculated at any time point using Eq. (14). For the implementation of the mathematical model, the programming language C++ was used (Borland C++ Builder V.6.0).

Fig. 8 shows examples for fittings of this "complex" mathematical model (solid curves) to experimentally determined metoprolol tartrate and PEG/PEO release profiles (symbols) from the investigated mini-matrices. For reasons of comparison, fittings of the above described "simple" mathematical model are also shown (dashed curves). It has to be pointed out that no additional parameter was fitted for the "complex" model, as the time-dependent system porosities were determined experimentally. Clearly, in all cases for which the "simple" model is not appropriate, much better agreement between the experimentally measured values and the theoretically calculated metoprolol tartrate and PEG/PEO release was achieved (Fig. 8a–d). The fact that there were still noteworthy deviations between the theory and the experiments can at least partially be attributed to the fact that crack formation (after about 4 h immersion in the release medium) sets on during drug release (Fig. 5d). This phenomenon is not taken into account in the mathematical modeling and can lead to underestimated drug release rates at late time points (the overestimation at early time points being a consequence of the fitting). Importantly, systems, which can be described by the "simple" model (e.g. Fig. 8b) can also be described by the "complex" model (with a similarly good agreement between theory and experiment). Thus, the "complex" model is applicable to a broad variety of mini-matrices, containing different amounts and types of PEG/PEO.

In order to evaluate the validity of the "complex" mathematical model, the latter was used to predict the resulting metoprolol concentration-position profiles within the mini-matrices at different time points. Fig. 9 shows an example for such a theoretical prediction. The concentration–position profile of metoprolol tartrate within a cross-section at $r = 0$ (Fig. 6) is shown in mini-matrices initially containing 2.5% PEO 100,000, which were exposed to the release medium for 24 h. Clearly, the drug concentration decreases in axial and radial direction from the centre of the cylinder. Importantly, still relatively high metoprolol tartrate concentrations (>200 mg/mL) are predicted close to the centre. Interestingly, these theoretical predictions could be confirmed by independent Raman measurements: Fig. 10 illustrates the metoprolol tartrate distribution in the mini-matrices, monitored via Raman using the 627–653 cm^{-1} spectral band as no overlap with Raman signals from the other tablet ingredients occurred at this spectral range. Based on the intensity of the Raman signal across the scanned sections of the mini-matrices, it was confirmed that metoprolol tartrate is homogeneously distributed in the mini-matrix before exposure to the release medium, since the metoprolol tartrate intensities were similar in the centre and at the edges of the mini-matrices, for $z = Z$ (exterior surface) and $z = 0$ (half height). After exposure to the release medium (24 h), surprisingly, a lower drug concentration

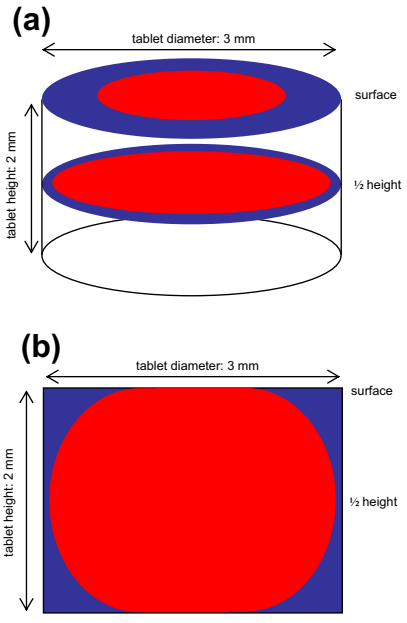

Fig. 10. Schematic drawing of the experimentally determined (Raman spectroscopy) metoprolol tartrate concentration profiles within mini-matrices (initially containing 2.5% PEO 100,000): (a) after 24 h exposure to the release medium – exterior surface and radial cutting surface (see also Fig. 1a) and (b) after 24 h exposure to the release medium – axial cutting surface (see also Fig. 1b). The metoprolol tartrate distribution in the mini-matrices is schematically presented via a binary colour code (blue indicating an area with low drug concentration, red indicating an area with high drug concentration). (For interpretation of the references to colour in this figure legend, the reader is referred to the web version of this article.).

was only detected at the tablet edges, whereas even at the exterior surface, the centre still contained high metoprolol tartrate concentrations (Fig. 10a). However, mapping of the axial cutting surface (Fig. 10b) showed that metoprolol tartrate preferentially diffused in the axial direction during dissolution. This can be explained by the fact that during hot-melt extrusion, the polymers are oriented parallel to the extrusion flow, resulting in a preferential diffusion route for drug release. This observation is in agreement with the anisotropic swelling due to axial relaxation of the polymers [17]. In addition, a drug particle will select the shortest diffusion path length to the release medium; since the height of our tablets is 2 mm in comparison with a diameter of 3 mm, the axial route is followed (especially of great importance for particles at the centre of the tablet).

4. Conclusions

The proposed mathematical theories allow for a better understanding of the underlying drug release mechanisms in hot-melt extruded mini-matrices, which strongly depend on the initial system composition. Importantly, the theories also allow for the quantitative prediction of the effects of formulation parameters on the resulting drug release kinetics and thus, for a facilitated optimization of this type of advanced drug delivery systems.

References

[1] W. Mueller, R. Spengler, S. Grabowski, A. Sanner, Feste pharmazeutische Retardforme. European Patent 0 544 144 B1, BASF Aktiengesellschaft; 1992.
[2] M. Fukuda, N.A. Peppas, J.W. McGinity, Properties of sustained release hot-melt extruded tablets containing chitosan and xanthan gum, Int J Pharm 310 (2006) 90–100.
[3] M. Fukuda, N.A. Peppas, J.W. McGinity, Floating hot-melt extruded tablets for gastroretentive controlled drug release system, J Control Release 115 (2006) 121–129.
[4] S.U. Schilling, C.D. Bruce, N.H. Shah, A.W. Malick, J.W. McGinity, Citric acid monohydrate as a release-modifying agent in melt extruded matrix tablets, Int J Pharm 361 (2008) 158–168.
[5] J.W. McGinity, J.J. Koleng, M.A. Repka, F. Zhang, Hot-melt extrusion technology, in: J. Swarbrick, J.C. Boylan (Eds.), Encyclopedia of pharmaceutical technology, vol. 19, Marcel Dekker, New York, 2001, pp. 203–226.
[6] J. Breitenbach, Melt extrusion: from process to drug delivery technology, Eur J Pharm Biopharm 54 (2) (2002) 107–117.
[7] J. Albers, R. Alles, K. Matthée, K. Knop, J.S. Nahrup, P. Kleinebudde, Mechanism of drug release from polymethacrylate-based extrudates and milled strands prepared by hot-melt extrusion, Eur J Pharm Biopharm 71 (2009) 387–394.
[8] Y. Zhu, N.H. Shah, A.W. Malick, M.H. Infeld, J.W. McGinity, Solid-state plasticization of an acrylic polymer with chlorpheniramine maleate and triethyl citrate, Int J Pharm 241 (2002) 301–310.
[9] C.R. Young, J.J. Koleng, J.W. McGinity, Production of spherical pellets by a hot-melt extrusion and spheronization process, Int J Pharm 242 (2002) 87–92.
[10] C. Wu, J.W. McGinity, Influence of methylparaben as a solid-state plasticizer on the physicochemical properties of Eudragit® RS PO hot-melt extrudates, Eur J Pharm Biopharm 56 (2003) 95–100.
[11] N. Follonier, E. Doelker, E.T. Cole, Evaluation of hot-melt extrusion as a new technique for the production of polymer based pellets for sustained release capsules containing high loadings of freely soluble drugs, Drug Dev Ind Pharm 20 (8) (1994) 1323–1339.
[12] N. Follonier, E. Doelker, E.T. Cole, Various ways of modulating the release of diltiazem hydrochloride from hot-melt extruded sustained release pellets prepared using polymeric materials, J Control Release 36 (1995) 243–250.
[13] G.P. Andrews, D.S. Jones, O.A. Diak, C.P. McCoy, A.B. Watts, J.W. McGinity, The manufacture and characterisation of hot-melt extruded enteric tablets, Eur J Pharm Biopharm 69 (2008) 264–273.
[14] C. De Brabander, C. Vervaet, J.P. Remon, Development and evaluation of sustained release mini-matrices prepared via hot-melt extrusion, J Control Release 89 (2) (2003) 235–247.
[15] C. De Brabander, C. Vervaet, L. Van Bortel, J.P. Remon, Bioavailability of ibuprofen from hot-melt extruded mini-matrices, Int J Pharm 271 (2004) 77–84.
[16] W.M. Van Den Abeele, C. De Brabander, C. Vervaet, J.P. Remon, L.M. Van Bortel, Bioavailability of ibuprofen from hot-melt extruded mini-matrices, Brit J Clin Pharmacol 57 (3) (2004) 366–367.
[17] E. Verhoeven, C. Vervaet, J.P. Remon, Xanthan gum to tailor drug release of sustained-release ethylcellulose mini-matrices prepared via hot-melt extrusion: in vitro and in vivo evaluation, Eur J Pharm Biopharm 63 (2006) 320–330.
[18] E. Verhoeven, T.R.M. De Beer, G. Van den Mooter, J.P. Remon, C. Vervaet, Influence of formulation and process parameters on the release characteristics of ethylcellulose sustained-release mini-matrices produced by hot-melt extrusion, Eur J Pharm Biopharm 69 (2008) 312–319.
[19] E. Verhoeven, T.R.M. De Beer, E. Schacht, G. Van den Mooter, J.P. Remon, C. Vervaet, Influence of polyethylene glycol/polyethylene oxide on the release characteristics of sustained-release ethylcellulose mini-matrices produced by hot-melt extrusion: in vitro and in vivo evaluation, Eur J Pharm Biopharm 72 (2009) 463–470.
[20] M.M. Crowley, B. Schroeder, A. Fredersdorf, S. Obara, M. Talarico, S. Kucera, J.W. McGinity, Physicochemical properties and mechanism of drug release from ethyl cellulose matrix tablets prepared by direct compression and hot-melt extrusion, Int J Pharm 269 (2004) 509–522.
[21] J. Siepmann, F. Siepmann, Mathematical modeling of drug delivery, Int J Pharm 364 (2008) 328–343.
[22] J. Siepmann, N.A. Peppas, Modeling of drug release from delivery systems based on hydroxypropyl methylcellulose (HPMC), Adv Drug Deliver Rev 48 (2001) 139–157.
[23] J. Siepmann, A. Göpferich, Mathematical modeling of bioerodible, polymeric drug delivery systems, Adv Drug Deliver Rev 48 (2001) 229–247.
[24] S. Herrmann, G. Winter, S. Mohl, F. Siepmann, J. Siepmann, Mechanisms controlling protein release from lipidic implants: effects of PEG addition, J Control Release 118 (2007) 161–168.
[25] S. Herrmann, S. Mohl, F. Siepmann, J. Siepmann, G. Winter, New insight into the role of polyethylene glycol acting as protein release modifier in lipidic implants, Pharm Res 24 (2007) 1527–1537.
[26] F. Siepmann, S. Herrmann, G. Winter, J. Siepmann, A novel mathematical model quantifying drug release from lipid implants, J Control Release 128 (2008) 233–240.
[27] J. Siepmann, F. Siepmann, A.T. Florence, Local controlled drug delivery to the brain: mathematical modeling of the underlying mass transport mechanisms, Int J Pharm 314 (2006) 101–119.
[28] J. Crank (Ed.), The mathematics of diffusion, 2nd ed., Clarendon Press, Oxford, 1975.
[29] J.M. Vergnaud, Controlled drug release of oral dosage forms, Ellis Horwood, New York, 1993.
[30] J.M. Vergnaud (Ed.), Liquid transport processes in polymeric materials, Prentice-Hall, Englewood Cliffs, 1991.